Analyst

Cite this: *Analyst*, 2012, **137**, 3502

www.rsc.org/analyst

PAPER

A molecularly imprinted photonic polymer sensor with high selectivity for tetracyclines analysis in food

Li-Qing Wang, Fan-Yan Lin and Li-Ping Yu*

Received 20th February 2012, Accepted 11th May 2012
DOI: 10.1039/c2an35460h

A molecularly imprinted photonic polymer (MIPP) sensor for respective detection of tetracycline, oxytetracycline and chlortetracycline is developed based on the combination of a colloidal crystal templating method and a molecular imprinting technique. Colloidal crystal templates are prepared from monodisperse polystyrene colloids. The molecularly imprinted polymer, which is embodied in the colloidal crystal templates, is synthesized with acrylic acid and acrylamide as monomers, *N*,*N*′-methylene bisacrylamide as a cross-linker and tetracyclines (TCs) as imprinting template molecules. After removal of the colloidal crystal template and the molecularly imprinted template, the resulted MIPP consists of a three-dimensional, highly ordered and interconnected macroporous array with a thin hydrogel wall, where nanocavities complementary to analytes in shape and binding sites are distributed. The response of MIPP to TCs stimulants in aqueous solution is detected through a readable Bragg diffraction red-shift, which is due to the lattice change of MIPP structures responding to their rebinding to the target TCs molecules. A linear relationship was found between the $\Delta\lambda$ and the concentration of TCs in the range from 0.04 μM to 0.24 μM. With this sensory system, direct and selective detection of TCs has been achieved without using label techniques and expensive instruments. The developed method has been applied successfully to detect tetracycline in milk and honey samples.

Introduction

Tetracyclines (TCs) are broad-spectrum antibiotics, which are usually employed as anti-infection agents and growth promoters in animal husbandry. Among them, tetracycline (TC), oxytetracycline (OTC), chlortetracycline (CTC) and doxycycline (DC) are the most widely used.[1] The widespread use of these TCs has become a serious problem since they may leave residues in products that can either be toxic or cause allergic reactions in some hypersensitive individuals, as well as promote the occurrence of antimicrobial-resistant bacteria.[2] The presence of veterinary drug residues in food has become an issue of intense international concerns and debates regarding risk assessment in recent years.[3] Many countries and groups have defined the maximum residue limits for TCs in various foods to ensure the safety of food for consumers. For example, the European Union has set maximum residue limits for TCs at 0.3 mg kg^{-1} in liver, 0.1 mg kg^{-1} in milk or muscle tissues, and 0.01 mg kg^{-1} in honey.[1] Therefore, it is of fundamental importance to determine the concentration level of TCs in food products in order to reduce problems during processing as well as to prevent their transmission to the consumers.

TCs are usually determined by microbiological methods,[4] immunoassay,[5] capillary electrophoresis,[6] and chromatography with ultraviolet,[7] spectrofluorometric,[8] and electrochemical detection.[9] The microbiological assay is usually used for the measurement of TCs in food because it is easy to perform and inexpensive. However, this method is complicated, time-consuming and lacks specificity.[4] Immunoassay is usually quite expensive. Instrumental analysis methods such as liquid chromatography are sensitive and highly specific but require expensive equipment, large volume of solvents and complicated clean-up procedures. Therefore, the development of simple, cheap, easy and selective methods for the determination of TCs is necessary for food safety.

Molecular imprinting is a powerful technique that is gaining attention for its prospect of creating synthetic polymers with highly specific recognition capabilities. So far, the molecular imprinting technique has been proven to be a powerful tool for selective recognition of TCs in complicated samples.[10–14] Molecularly imprinted polymers are synthetic polymeric materials with specific recognition sites complementary in shape, size and functional groups to the template molecule, including an interaction mechanism based on molecular recognition.[15] Several factors should be considered in designing molecularly imprinted polymers. The polymers must have sufficient mechanical stability to withstand the manipulation. The structure of the polymers needs to be rigid enough to retain a permanent memory of the imprint, and the polymers need to be macro-porous to allow the template molecules to diffuse in and out easily.[10] Generally, molecular imprinting recognition and separation is based on

Department of Chemistry, School of Science, Tianjin University, Tianjin 300072, China. E-mail: lipingyu@tju.edu.cn; Fax: +86-22-27403475

bulk polymers, which have the disadvantages of restricting mobility of the analyte molecules within highly cross-linked polymer networks and poor efficiency in binding due to long diffusion paths and the absence of accessible cavities for the analytes in the bulk. To solve those problems concerning the molecular imprinting technique, efforts such as surface molecular imprinting strategy,[16] molecular imprinting on porous supports,[17] molecular imprinting nanotechnologies,[18] and porous molecularly imprinted polymer strategies[19] have been proposed. In addition, for assays with a traditional molecular imprinting technique, the analyte must contain a chromophore or a fluorophore, or be electroactive to generate a readable optical or electronic signal. Otherwise, the analyte must be modified or tagged. Thus far, there are no reports for direct detection and quantification of TCs that is simply through a readable optical signal to TCs rebinding events in the molecular imprinting process.

Lately, a new molecularly imprinted photonic polymer (MIPP) based on the combination of colloidal crystal templating and molecular imprinting technique has been developed.[20–24] This approach involves the formation of complexes between the imprinting molecule and hydrogel functional monomers based on relatively weak, non-covalent interactions on a colloidal crystal template.[20] Colloidal crystal templating has been used to create highly ordered, three-dimensional (3D), inverse opal photonic crystal structures after the removal of colloidal particles, which retain the opal characteristics of the original lattice of the photonic crystal.[25–30] Hydrogel films of inverse opal structure display a tunable optical response sensitive to pH value,[24,26] glucose[25] and humidity.[27] After removal of two templates (the colloidal crystal template and the molecularly imprinted template), the resulted MIPP can accommodate a 3D, highly ordered and interconnected macropore array with a thin hydrogel wall, in which nanocavities complementary to analytes in shape and binding sites are distributed. Owing to the periodic porous structure, such inverse opal materials exhibit fascinating optical properties of photonic crystals such as Bragg diffraction and/or bright structural color. The presence of macropores in MIPP provides more interaction sites, and can also offer increased mass transport and easier accessibility to the active sites through the material. The porous hydrogels exhibit rapid swellings or shrinkage in volume responding to chemical stimuli. The additional nanocavities, deriving from molecular imprinting, make these hydrogels highly specific to analytes. Meanwhile, the change of the periodic lattice spacing of the 3D ordered photonic polymer films can give rise to interesting optical properties, which can be used to optically determine analytes by means of the shift of the Bragg diffraction.[20–34] Thus, MIPP is promising in developing molecular sensors that can not only exhibit high specificity, sensitivity, and quick response, but also be detected directly and easily without using label techniques and expensive instruments.[20–24]

MIPP was introduced and then has been further developed by Li's group.[20–24] Their achievements to date including recognitions of L-dopa,[20] protein,[21] cholic acid,[22] alkaloids[23] and atrazine[24] demonstrate a very promising sensor platform of MIPP. However, the development of a MIPP-based sensor is still in its initial stage. In Li's work,[20–24] monodisperse silica spheres were used to form a colloidal crystal template and methacrylic acid (MA) as a functional monomer, ethylene glycol dimethylacrylate (EGDMA) as a cross-linker and 2,2′-azoisobutyronitrile (AIBN) as an initiator were chosen. Their MIPP was photopolymerized in an ice bath and PMMA slides were used to support the obtained MIPP film. In our work, a MIPP imprinting system for TCs molecules was developed. In general, it is hard to find a suitable system for every template molecule where the binding is strong enough to make acceptable cavities yet easily cleavable to achieve fast and easy extraction of the template from the network. The performance of a MIPP is dependent on the initial choice of polymerizable ingredients and the reaction conditions that are used to synthesize the polymer. With the desired properties in mind, we carefully selected the monomer species, their concentrations and ratio, the concentration of cross-linker, the backfilling technique of precursors, the way of polymerization and the conditions of templates removal for making the MIPP, which are different from the work developed by Li's group.

TC, OTC, and CTC are chosen as imprinting template molecules in our present work. Monodisperse polystyrene (PS) colloids are used to self-assemble into a colloidal crystal template. An optimal molecular imprinting system for TCs is chosen, including acrylamide and acrylic acid as monomers, *N*,*N*′-methylene bisacrylamide as a cross-linker and ammonium persulfate as an initiator. MIPP is synthesized by a thermal polymerization in the PS colloidal crystal template which is infiltrated with a mixture of precursors. After the removal of templates, an inverse opal structure is created in our MIPP and its sensor characters are tested under various TCs concentrations. The optical changes of the Bragg diffraction peak resulting from the response of the target TCs molecules are detected directly by a fiber optic spectrometer. MIPP sensing for TCs with direct, sensitive and label-free detection has been achieved without any sample pre-treatment and expensive instruments. Sensitivity and specificity of responses to TCs stimulants of the MIPP sensor have been investigated. The proposed sensor has been applied to the analysis of TC residues in milk and honey samples.

Experimental section

Materials

Tetracycline hydrochloride (TC) was purchased from Alfa Aesar. Oxytetracycline hydrochloride (OTC) and 4-epichlorotetracycline hydrochloride (CTC) were purchased from Aladdin Reagent (Shanghai, China). The chemical structures of above TCs are reported in Fig. 1. TC, OTC, and CTC stock solutions were prepared in deionized water and the standard solutions of lower concentrations were prepared by diluting the stock solutions. All stock solutions were protected from light and re-prepared every week. Acetic acid, styrene, sodium dodecyl sulfonate (SDS), ammonium persulfate (APS), acrylamide (AMD), acrylic acid (AA), *N*,*N*′-methylene bisacrylamide (BIS) and other affiliated chemicals were all from local suppliers. Styrene was vacuum distilled to remove inhibitors prior to use, and other solvents and chemicals were of reagent quality and were used without further purification unless specially mentioned. All containers and glass slides (50 × 20 mm) for

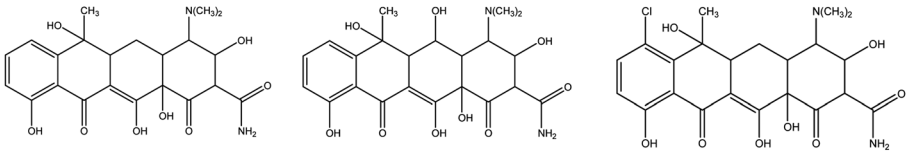

Fig. 1 Molecular structures of the three investigated tetracyclines.

colloidal crystal growth were cleaned by rinsing with a H_2SO_4–H_2O_2 mixture and deionized water.

Preparation of polystyrene (PS) colloidal crystal templates

The monodispersed PS colloids with different diameters were synthesized by emulsion polymerization in the same way as in ref. 29 and 30. Templates of colloidal crystal were prepared from the obtained monodispersed PS colloids by using the vertical deposition method.[29,30] PS colloid particles in aqueous media with a concentration of about 5% (v/v) were placed into treated containers. A treated glass slide was put into each container vertically for colloidal crystal growth. Containers were placed in a 43 °C water bath for 2–3 days. After the solvent was evaporated completely, templates of close-packed face-centered cubic (fcc) colloidal crystals were obtained.

Preparation of a tetracycline MIPP film

AMD and AA were both used as monomers. Prior to infiltration into the voids of the PS colloidal crystal, AMD and AA were mixed with TCs in water for sufficient intermolecular interaction to form a stable complex. Appropriate amounts of BIS as a cross-linker and APS as an initiator were added. Following a sufficient homogenization, the mixture of precursors was infiltrated into the above PS colloidal crystal template by using a capillary-attraction-induced method and the interstitial space between the close-packed spheres was filled with the solution because of the capillary effects. After polymerization in an oven at 60 °C for 3 hours, the template was firstly immersed in dimethylbenzene to completely remove the PS colloidal crystal template, then washed with a 10% (v/v) acetic acid containing 10% (w/v) SDS solution to remove the TCs templates in a bath oscillator at 75 °C for 2 hours and rinsed thoroughly with deionized water until no further diffraction changes were observed, indicating full removal of TCs from the imprinted films. A transparent thin film of TCs MIPP was obtained. The corresponding non-molecularly imprinted photonic polymer (NIPP) was prepared in the same way but the TCs molecules template was excluded from the procedure.

Characterization

Surface morphologies of the used templates and the imprinted films were observed by a field-emission scanning electron microscope (JEOL JSM-6700, Japan) operating at 25 kV. The colors of the colloidal crystal templates and MIPP films were recorded by using a Canon PowerShot SX20 IS digital camera.

Determination of MIPP to recognition

The optical responses of the MIPP film to TCs were measured in buffer solutions of various TCs by using a 380–1050 nm fiber optic spectrometer (JKHQ-D1, Tianjin, China) in the vertical direction. The fiber optic spectrometer is convenient to fix the same measurement location on the film by focusing the incident light on one dot. And always a maximum diffraction peak is observed in our experiments. Before each spectral scan, the pH of all solutions was checked and the final pH value was adjusted in the range of 5 to 7. In all cases, the MIPP film was soaked in 10 mL buffer solutions of various chemicals for 5 minutes at room temperature until it reached a swelling equilibrium. After one detection, the film was soaked again in a 10% (v/v) acetic acid containing 10% (w/v) SDS solution for 30 minutes and then rinsed thoroughly with deionized water to recover the blank state for the next detection. For a series of TCs concentrations, the detection followed the sequence from low to high concentrations to eliminate interference.

Preparation of spiked samples

The milk and honey samples were purchased from local markets. Milk was used without further treatment and honey was dissolved in buffer water. Spiked samples were prepared by adding TC standard solution into honey and milk solution with a final concentration of 0.08 μM and 0.12 μM respectively; the total volumes of both are 10 mL and the final pH value was checked and maintained in the range of 5 to 7. The diffraction spectra of the MIPP film in buffer water were first measured and then the MIPP film was immersed into the analyte aqueous solution at room temperature for 5 minutes before sample testing.

It should be noted that the MIPP film produced in our work is robust enough to go through a series of tests. Conditions under which the sensor is allowed to be dried and rehydrated while retaining its diffraction and sensing properties have been demonstrated, and a single MIPP film was used throughout a sequent investigation to minimize variations and errors.

Results and discussions

Fabrication of a tetracycline imprinted photonic polymer

Fig. 2 displays the four-step approach employed for the construction of a TCs imprinted photonic polymer, including the preparation of the colloidal crystal template by using the vertical deposition method as shown in Fig. 2a, the infiltration of liquid precursors and the complex of TCs with monomers into the voids of the colloidal crystal template by using a capillary-attraction-induced method as shown in Fig. 2b, the polymerization without

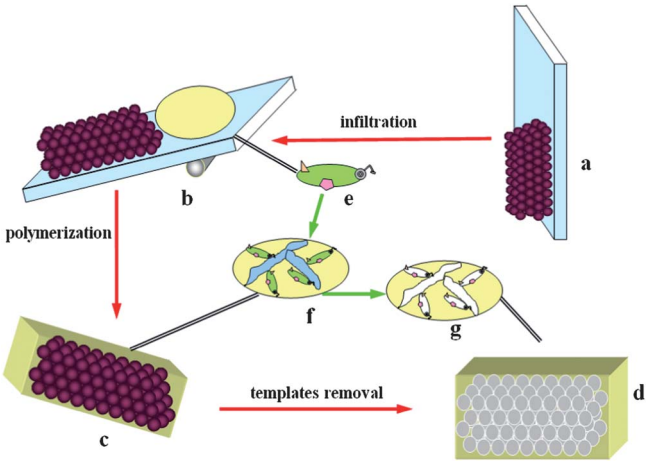

Fig. 2 Protocol for the preparation of MIPP films: (a) PS colloids self-assembled into colloidal crystals on a glass substrate; (b) infiltration of complex solution into a colloidal crystal template; (c) polymerization of a TCs imprinted photonic polymer; (d) MIPP film after the removal of the PS colloidal crystal template and TCs imprinted molecule template; (e) complex of the monomer and imprinted template molecule; (f) imprinted molecules within the polymer networks and (g) imprinted cavities with complementary shape and binding sites to the template molecule.

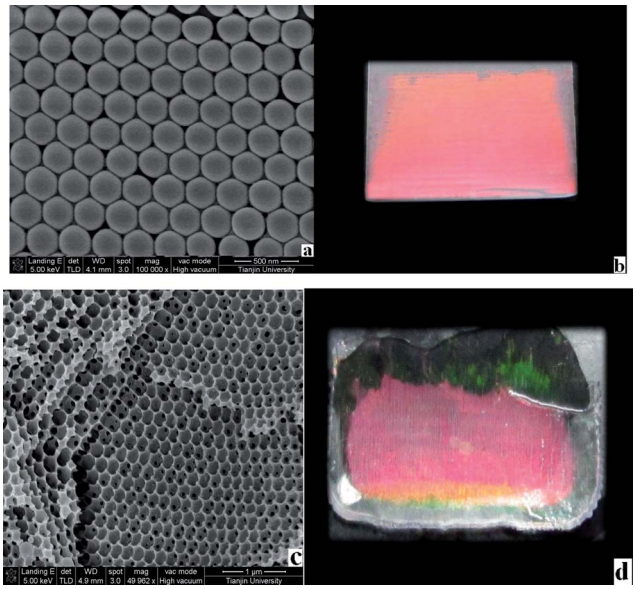

Fig. 3 Typical SEM image (a) and photograph (b) of the used PS colloidal crystal template, and typical SEM image (c) and photograph (d) of the resulting MIPP film.

elution of both the TCs templates and the colloidal crystal template (Fig. 2c), and the removal of the used colloidal crystal template and the imprinted molecule template (Fig. 2d). During each of the processing steps, it is possible to introduce additional defects, and template materials suitable for backfilling and removal without pattern collapse are rather important. However, the slight heterogeneity produced by unavoidable defects in the preparation process is not serious because complete photonic bandgaps of photonic crystal structures are not required in chemical/biological and optical sensors.[35]

Colloidal assembly is a low cost and low-energy consumption method to fabricate 3D photonic structures. The method is based on the self-assembly of monodispersed colloidal particles into an ordered crystalline structure. In the present work, a highly ordered close-packed structure of the colloidal crystal templates is formed by self-assembly of monodisperse PS particles in deionized water. In the case of the vertical deposition, the solvent from the colloidal solution is evaporated by controlling the temperature gradient. In the present work, monodispersed PS particles with a diameter of about 200 nm were used to form a colloidal crystal template. Fig. 3a shows the top view of a PS colloidal crystal template. It is clearly seen that the PS colloidal crystal possesses a face-centered cubic (fcc) close-packed structure with the (111) plane parallel to the substrate surface.

Different ratios of monomer, cross-linker, and imprinted template molecule have a considerable influence on the sensing properties of the imprinted photonic materials.[22] The preparation procedure of the MIPP is akin to the bulk molecular imprinting technique. However, the cross-linking density of the polymers in the conventional imprinting technique is extremely high, and the resulting imprinted polymer networks are hard resins and cannot undergo a large swelling change in response to guest molecules. In order to achieve the optimal conditions and to discover recipes for constructing the desired sensors, different ratios and contents of monomers and cross-linkers are explored in our study. When a higher ratio of cross-linker to monomer is used, a more fragile MIPP film will be obtained. Although a highly cross-linked rigid matrix is ideal for the formation of delicate recognition sites, the swelling and shrinkage capabilities of the formed MIPP film are strongly reduced and only small Bragg diffraction shifts are observed upon exposure to the target analytes. In contrast, a lower ratio of cross-linker to monomer can afford a more flexible MIPP film. Finally, the MIPP film is prepared by placing the template (TCs, 0.015 mmol) in a glass container with the monomer (42 mmol, 67 mol% AMD and 19 mmol, 31 mol% AA), cross-linker (0.6 mmol, 0.9 mol% BIS) and initiator (0.4 mmol, 0.6 mol% APS), all dissolved in 4 mL of aqueous solution. After polymerization and removal of templates, the resulted MIPPs have not only a well-defined 3D ordered macroporous structure and a large internal surface area, but also a number of cavities with complementary shape and binding sites left by the imprinted molecules as shown in Fig. 3c. Both the periodically ordered opal structure of the PS colloidal crystal template and the inverse opal structure of the MIPP film can exhibit brilliant structural color as shown in Fig. 3b and d since their Bragg diffraction is located in the visible-light region.

Response speed of MIPP

As for the designs of sensors, a rapid response to the external environment is an important factor. The ordered and interconnected macroporous hydrogel structure endows the MIPP film with a rapid response to external stimuli. Porous structures increase the surface-to-volume ratio, allowing faster diffusion into the hydrogel polymer. It is so easy for analytes to diffuse and move from bulk solution to recognition sites through the interconnected macropores that the photonic hydrogel film can

quickly generate signals and reach equilibrium upon exposure to stimuli. For small molecules, Hu *et al.* observed a response time of several seconds.[21] The interval of time required for the volume of a hydrogel to change is governed by the collective diffusion of the polymer network forming the MIPP. A bulk hydrogel polymer exhibits poor analyte accessibility and mass transport,[36,37] because its dense polymer skin layer prevents the permeability of solvent molecules when the environment changes drastically.[36] In contrast to the bulk hydrogel, the porous MIPP exhibits a very short response time, which is attributed to the interconnecting porous structure that makes analyte diffusion easier. In this work, the chosen soaking time of 5 minutes for any concentration of TCs is sufficient for diffusion and swelling equilibrium to occur, hence no further diffraction changes have been observed.

Sensing properties of MIPPs to TCs

Three kinds of TCs (TC, OTC, and CTC) that are structurally similar (Fig. 1) are chosen as the template molecules and their responses to different MIPPs have been compared in order to reveal the specificity in the molecular-imprinting process. Herein, MIPP1, MIPP2 and MIPP3 are prepared using TC, OTC, and CTC respectively as the imprinted template.

After polymerizing the hydrogel polymer within the interstitial space of the colloidal crystal and removing two templates, the remaining inverse opal MIPP film has been excited by a variety of sensing phenomena depending on the chemical equilibrium between the analytes and the bound receptor. In our case, owing to the 3D ordered porous structure, the signal can be generated by the MIPP itself through Bragg diffraction, and the molecular recognition process can be directly transferred into readable optical signals. The diffraction response of TC imprinted MIPP1 film is observed by a fiber optic spectrometer. Fig. 4a exhibits the sensing behavior of the MIPP1 film responding to a series of concentrations of TC. It is found that the optical diffraction shift of MIPP1 is sensitive to the rebinding of TC molecules. The original Bragg diffraction wavelength of MIPP1 in buffer water is at 647 nm, and the MIPP1 film displays a 10 nm diffraction red-shift in the presence of 0.04 μM TC after being immersed into the solution for 5 minutes.

With the increase of the concentration of TC, the diffraction peak of MIPP1 red-shifts gradually and the total red-shift reaches about 150 nm until the TC concentration is 0.24 μM. Fig. 4b shows that there is a linear relationship between the $\Delta\lambda$ of the diffraction peak and the concentration of TC in the range from 0.04 μM to 0.24 μM. The molecular recognition group attached to the MIPP can actuate a volume increase proportional to the concentration of analytes, which results in a red-shift increase of the diffracted wavelength. Because the hydrogel volume is a function of analyte concentration, the diffraction shift from the hydrogel is a function of analyte concentration.[32] A linear equation $\Delta\lambda = 651.99c - 3.10$ with an R^2 of 0.9649 has been obtained for the linear relationship between the $\Delta\lambda$ of the diffraction peak and the concentration of TC. The MIPP1 should be able to resolve and sense a minimum TC concentration difference of 0.005 μM since the minimum differentiated diffraction wavelength of the fiber optic spectrometer is 0.23 nm.

Experiments of MIPP2 to OTC and MIPP3 to CTC have been performed respectively with the same preparation procedure. We find out that MIPP films are capable of detecting three kinds of corresponding TCs since shifts in the wavelength of diffracted light are all proportional to the concentration of analytes. Fig. 5a and b show that there are similar linear relationships between the $\Delta\lambda$ of the diffraction peak and the concentration of OTC and CTC in the range from 0.04 μM to 0.24 μM.

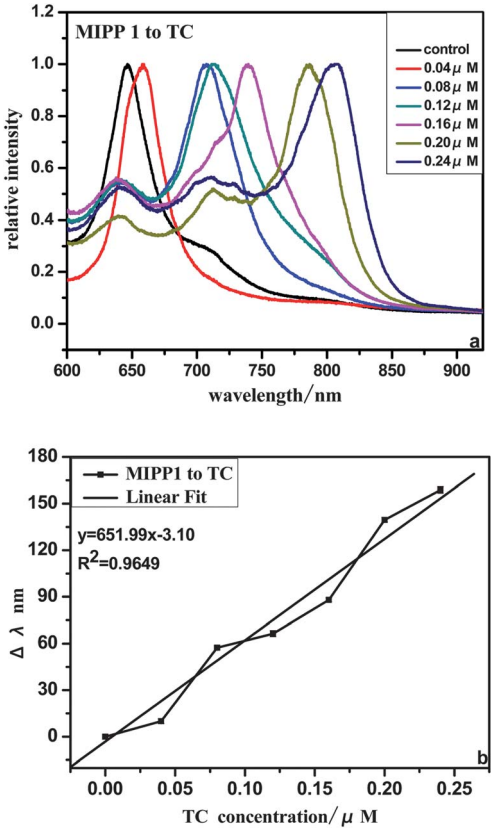

Fig. 4 (a) Diffraction response of MIPP1 to TC solution of varying concentrations. (b) Relationship between the $\Delta\lambda$ of diffraction peak and the concentration of TC in the range from 0.04 μM to 0.24 μM.

Selectivity of the MIPP film

The selectivity of this sensor depends on the recognition selectivity of the molecular imprinting technique. Molecularly imprinted polymers based on acrylic type polymers exhibit high selectivity and affinity towards the target compound.[37] To elucidate the molecular recognition properties of the imprinted materials, the optical response of the non-molecularly imprinted photonic polymer (NIPP) film without TC added is also investigated in various concentrations of TC as a control experiment. Fig. 6a shows that there is almost no diffraction peak shift of the NIPP film with the same concentration variation of TC. As shown in Fig. 6b, the same MIPP1 film has a regularly increasing red-shift when soaked in a series of concentrations of TC, but has a slight and irregular shift when soaked in the same variation of concentrations of OTC and CTC. All the results indicate that the microenvironments created by molecular imprinting are responsible for the observed responses of MIPP1 to TC, which elucidates that molecular imprinting plays a key role in the specific recognition of the MIPP film to the target molecule.

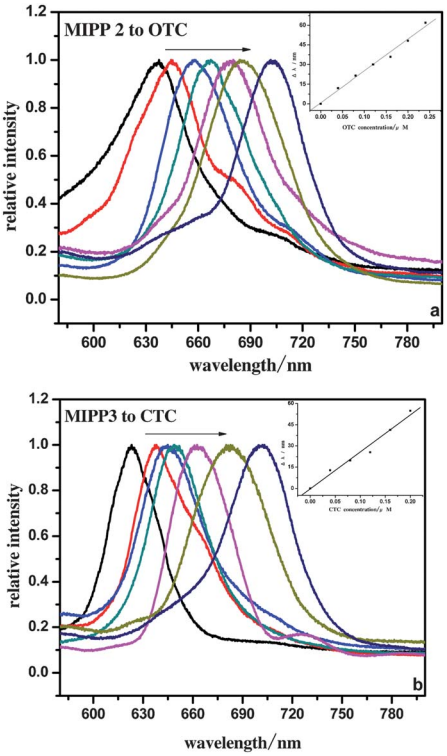

Fig. 5 (a) Diffraction response of MIPP2 to OTC and (b) MIPP3 to CTC solutions of varying concentrations. The inset is the fit relationship between the $\Delta\lambda$ of the diffraction peak and the concentration of TCs in the range from 0.04 μM to 0.24 μM.

MIPP2 imprinted by OTC and MIPP3 imprinted by CTC are also carried out to test the selectivity. Fig. 6c and d show the high specifcity of the prepared MIPP flms to the corresponding imprinted molecular in comparison to other similar structures. The inherent affinity of the nanocavities resulted from molecular imprinting enables the MIPP film to recognize analytes highly

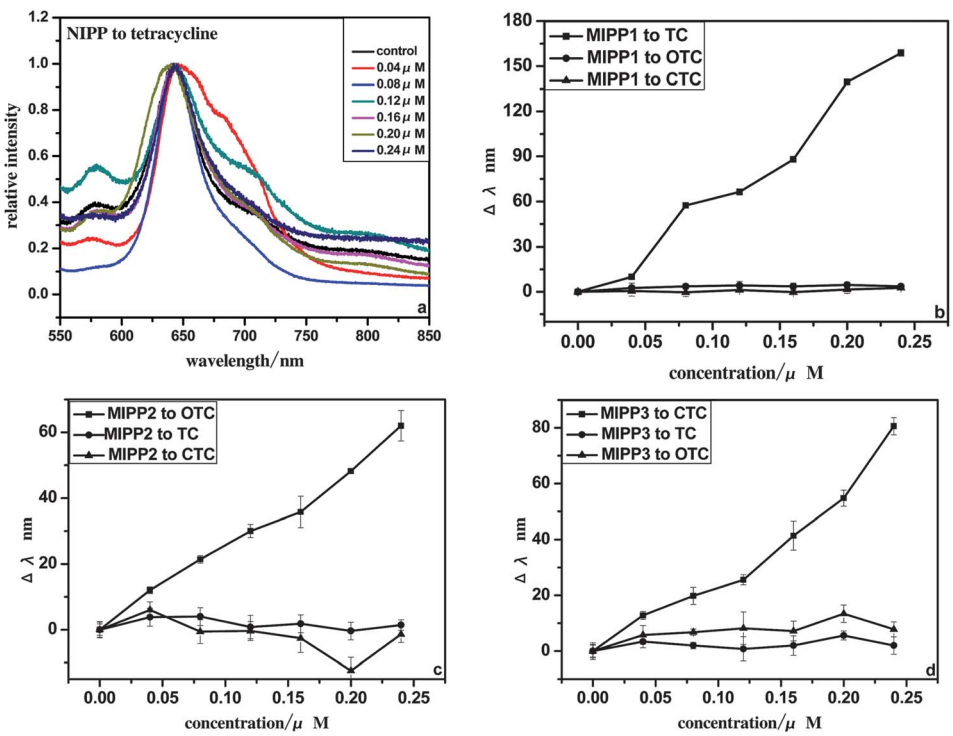

Fig. 6 (a) Response of NIPP to TC and response of MIPP1 (b), MIPP2 (c), and MIPP3 (d) to TC, OTC and CTC in the same variation of concentrations.

selectively. The fact that the prepared MIPP can discriminate the very similar TC molecules suggests that the cooperative effects of shape, size, and interaction sites of the formed binding sites play a critical role in the highly selective molecular recognition process of MIPP.

Usually, hydrogen bonding is essential for molecular recognition in aqueous media and hydrogen bond-based molecular imprints show specific recognition for small molecules in aqueous solutions. In our case, AA was chosen as a functional monomer due to its ready formation of hydrogen bonding with the template molecules. The interactions of the carboxylic groups of the polymer chain play an important role in the discrimination process.[38] TC is a rigid molecule (Fig. 1) with several hydroxyls and polar groups that allow the formation of strong hydrogen bonds with the carboxylic acid groups of the co-polymer. Dual hydrogen bonding is expected to occur between TCs and AA as a key interaction necessary for binding-site construction, in which a carboxylic group of AA works as both a hydrogen-bond acceptor and a donor that interacts with a hydrogen atom of the amino group and a nitrogen atom of the TC body, respectively. The possible establishment and interruption process of the hydrogen bonding between the functional monomer AA and TC template molecule is shown schematically in Fig. 7. The removal of the template from the imprinted polymer matrix affords both specific cavities which are topographically complementary to the template and binding sites arranged at the desired positions in the cavities which could subsequently interact with the hydroxyl groups of TCs through noncovalent interactions. Clearly, owing to the shape, size, and interaction sites in the formed binding sites, only target molecules can occupy the imprinted nanocavities within the MIPP network and cause a volume change in the MIPP film, thereby inducing a red-shift in the diffraction peak.

Previous studies have shown that even in a large molecule, one small group is important in the selective interactions that occur during recognition, either due to shape or to hydrogen bonding ability. Hydrogen bonding is believed to be the main interaction

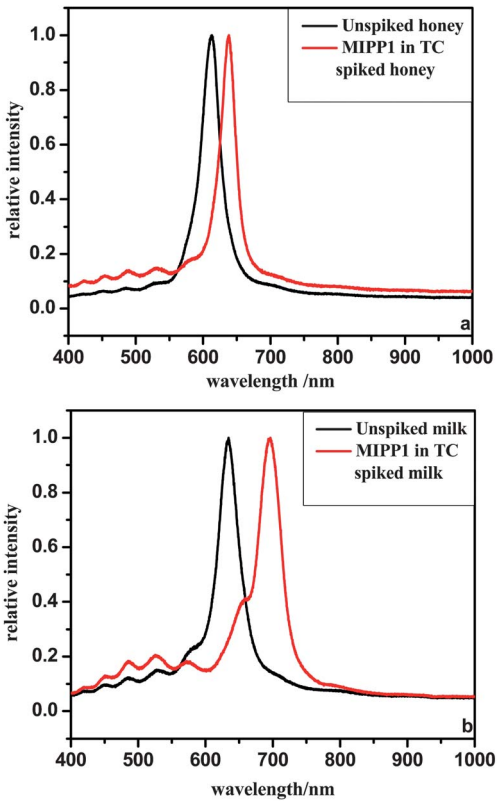

Fig. 8 Diffraction response of MIPP1 in the TC spiked honey (a) and milk (b) sample.

responsible for the retention of TCs by the imprinted polymer. Because hydroxyl groups could form hydrogen with a carboxylic group on the polymer, the difference in the structure and amount of OH and Cl groups among tetracycline, oxytetracycline and chlorotetracycline can result in differences in retention. So the imprinted polymers can recognize a very small difference among

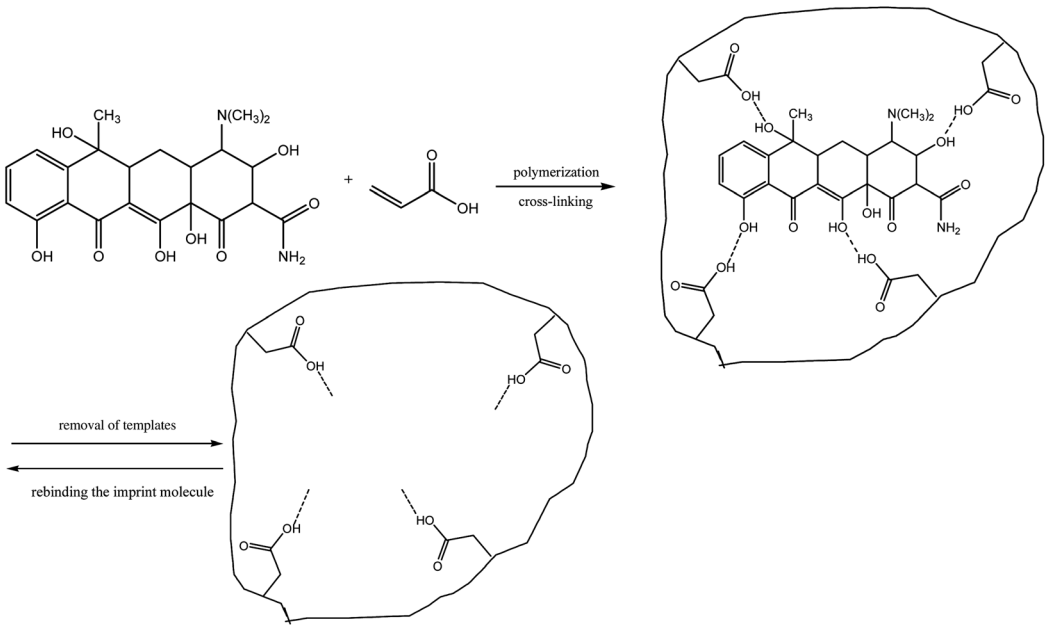

Fig. 7 The establishment and interruption process of the hydrogen bonding between the functional monomer AA and the TC template molecule.

tetracycline, oxytetracycline and chlorotetracycline depending on the imprinting mechanism of the molecular imprinting technique.

Applications

The developed method has been used to analyze samples purchased from the market. No shift of the diffraction peak is observed in the test sample because the content of TC in the purchased samples is below the limit of quantitation. Two MIPP1 films are soaked in honey and milk sample solution which are spiked with 0.08 μM and 0.12 μM TC respectively. The optical responses of MIPP1 to the unspiked sample and TC spiked samples are shown in Fig. 8. It is obvious that there is a significant red-shift of the diffraction peak both in milk and in honey. The application of the newly developed method makes the detection of significant amounts of persistent TC residuals in liquid sample possible.

Conclusions

In this paper, we have developed a new approach based on the combination of photonic crystal templating and molecular imprinting techniques, which is convenient to sense TCs in liquid samples. The imprinted film has a great advantage of having a rapid response which can be detected directly by a fiber optic spectrometer for its 3D macroporous structures introduced by the photonic crystal templates. The imprinted film also demonstrates much higher selectivity and sensitivity compared with the non-imprinted film, which is thought to be the result of the complementary shape, size, and nanocavities produced by the template molecule.

Acknowledgements

This work is supported by the National Natural Science Foundation of China (no. 20705023).

References

1 Z. Y. Guo and P. P. Gai, *Anal. Chim. Acta*, 2011, **688**, 197.
2 J. B. Ghasemi and A. R. Jalalvand, *Spectrochim. Acta Part A*, 2011, **78**, 277.
3 N. Vragović, D. Bažulić and B. Njari, *Food Chem. Toxicol.*, 2011, **49**, 352.
4 J. Kurittu, S. Lönnberg, M. Virta and M. Karp, *J. Agric. Food Chem.*, 2000, **48**, 3372.
5 M. Jeon and I. R. Paeng, *Anal. Chim. Acta*, 2008, **626**, 180.
6 S. Y. Wang, P. Yang and Y. Y. Cheng, *Electrophoresis*, 2007, **28**, 4173.
7 W. C. Andersen, J. E. Roybal, S. A. Gonzales, S. B. Turnipseed, A. P. Pfenning and L. R. Kuck, *Anal. Chim. Acta*, 2005, **529**, 145.
8 A. Pena, C. M. Lino, R. Alonso and D. Barceló, *J. Agric. Food Chem.*, 2007, **55**, 4973.
9 I. G. Casella and F. Picerno, *J. Agric. Food Chem.*, 2009, **57**, 8735.
10 W. S. Cai and R. B. Gupta, *Sep. Purif. Technol.*, 2004, **35**, 215.
11 F. Trottaa, C. Baggianib, M. P. Ludaa, E. Driolic and T. Massaria, *J. Membr. Sci.*, 2005, **254**, 13.
12 X. G. Hu, J. L. Pan, Y. L. Hu, Y. Huo and G. K. Li, *J. Chromatogr., A*, 2008, **1188**, 97.
13 L. G. Chen, J. Liu, Q. L. Zeng, H. Wang, A. M. Yu, H. Q. Zhang and L. Ding, *J. Chromatogr., A*, 2009, **1216**, 3710.
14 T. Jing, Y. Wang, Q. Dai, H. Xia, J. W. Niu, Q. L. Hao, S. R. Mei and Y. K. Zhou, *Biosens. Bioelectron.*, 2010, **25**, 2218.
15 V. Pichon and F. Chapuis-Hugon, *Anal. Chim. Acta*, 2008, **622**, 48.
16 S. F. Xu, J. H. Li and L. X. Chen, *J. Mater. Chem.*, 2011, **21**, 4346.
17 E. Yilmaz, K. Haupt and K. Mosbach, *Angew. Chem., Int. Ed.*, 2000, **39**, 2115.
18 G. J. Guan, B. H. Liu, Z. Y. Wang and Z. P. Zhang, *Sensors*, 2008, **8**, 8291.
19 S. F. Xu, L. X. Chen, J. H. Li, Q. Wei and J. P. Ma, *J. Mater. Chem.*, 2011, **21**, 12047.
20 X. B. Hu, Q. An, G. T. Li, S. Y. Tao and J. Liu, *Angew. Chem., Int. Ed.*, 2006, **45**, 8325.
21 X. B. Hu, G. T. Li, J. Huang, D. Zhang and Y. Qiu, *Adv. Mater.*, 2007, **19**, 4327.
22 Z. Wu, X. B. Hu, C. A. Tao, Y. Li, J. Liu, C. D. Yang, D. Z. Shen and G. T. Li, *J. Mater. Chem.*, 2008, **18**, 5452.
23 X. B. Hu, G. T. Li, M. H. Li, J. Huang, Y. Li, Y. B. Gao and Y. H. Zhang, *Adv. Funct. Mater.*, 2008, **18**, 575.
24 Z. Wu, C. A. Tao, C. X. Lin, D. Z. Shen and G. T. Li, *Chem.–Eur. J.*, 2008, **14**, 11358.
25 Y.-J. Lee and P. V. Braun, *Adv. Mater.*, 2003, **15**, 563.
26 Y.-J. Lee, S. A. Pruzinsky and P. V. Braun, *Langmuir*, 2004, **20**, 3096.
27 J. Shin, P. V. Braun and W. Lee, *Sens. Actuators, B*, 2010, **150**, 183.
28 R. A. Barry and P. Wiltzius, *Langmuir*, 2006, **22**, 1369.
29 J. Y. Wang, Y. Cao, Y. Feng, F. Yin and J. P. Gao, *Adv. Mater.*, 2007, **19**, 3865.
30 Y. Liu, Y. X. Yuan, J. K. Ma, Y. Liu, L. Cui, R. G. Huang and J. P. Gao, *J. Mater. Chem.*, 2011, **21**, 19233.
31 J. H. Holtz, J. S. W. Holtz, C. H. Munro and S. A. Asher, *Anal. Chem.*, 1998, **70**, 780.
32 C. E. Reese, M. E. Baltusavich, J. P. Keim and S. A. Asher, *Anal. Chem.*, 2001, **73**, 5038.
33 M. Ben-Moshe, V. L. Alexeev and S. A. Asher, *Anal. Chem.*, 2006, **78**, 5149.
34 J. P. Walker, K. W. Kimble and S. A. Asher, *Anal. Bioanal. Chem.*, 2007, **389**, 2115.
35 J. H. Moon and S. Yang, *Chem. Rev.*, 2010, **110**, 547.
36 D. Nakayama, Y. Takeoka, M. Watanabe and K. Kataoka, *Angew. Chem., Int. Ed.*, 2003, **42**, 4197.
37 Elmer-Rico E. Mojica, J. Autschbach, F. V. Bright and D. S. Aga, *Analyst*, 2011, **136**, 749.
38 F. Trottaa, C. Baggianib, M. P. Ludaa, E. Driolic and T. Massaria, *J Membr. Sci.*, 2005, **254**, 13.